

Inclusion Complex Formation of Thiacalix[4]arene and Xe in Aqueous Solution Studied by Hyperpolarized ^{129}Xe NMR

JUNKO FUKUTOMI*, YUKO ADACHI, AKARI KANEKO, ATSUOMI KIMURA and HIDEAKI FUJIWARA*

Division of Health Sciences, Graduate School of Medicine, Osaka University, 1-7 Yamadaoka, Suita, Osaka, 565-0871, Japan

(Received: 26 May 2006; in final form: 10 July 2006)

Key words: calixarene, enthalpy, entropy, hyperpolarized, inclusion complex of Xe

Abstract

The inclusion complex formation of 4-sulfothiacalix[4]arene sodium salt (STCAS) and Xe has been investigated by using hyperpolarized ^{129}Xe NMR spectroscopy. Our new continuous-flow type hyperpolarizing system has advantageous capabilities that can supply hyperpolarized gases continuously and directly to a sample solution in a NMR tube. Consequently saturated Xe concentration in the aqueous solution of STCAS is maintained during the NMR experiment, and ^{129}Xe NMR spectra can be obtained in remarkably short time. STCAS concentration dependence of ^{129}Xe chemical shift has been analyzed in an elaborated way by a computer method as well as a simple graphic method that we have proposed. The association constant $K: 13.6 \pm 0.8 \text{ M}^{-1}$ at 25°C was obtained, and further analysis of the temperature dependence has successfully given thermodynamic parameters of enthalpy (ΔH) and entropy (ΔS) for the inclusion complex formation: $\Delta H = -11.9 \pm 1.9 \text{ kJ mol}^{-1}$ and $\Delta S = -17.4 \pm 5.8 \text{ JK}^{-1} \text{ mol}^{-1}$. The energetic aspects of complex formation are discussed from the size effect and from the molecular theory of standard entropy, and a release of definite number of water molecules from STCAS cavity is suggested in the inclusion complex formation with Xe.

Abbreviations: FID: Free Induction Decay; HP: Hyperpolarized; NMR: Nuclear Magnetic Resonance; PSAS: *p*-phenolsulfonic acid sodium salt; RF: Radio-Frequency; SPINOE: Spin Polarization-Induced Nuclear Overhauser Effect; STCAS: 4-Sulfothiacalix[4]arene sodium salt.

Introduction

As may be seen in an occurrence of new concept of molecular mechanisms of general anesthesia [1] that anesthetics affect directly protein by binding to pockets or clefts, molecular recognition has been stimulated to the center of interest in supramolecular chemistry [2]. Xenon, a chemically inert element, has long been known to act as a general anesthetic, and used as a probe for structural and dynamic profiles in host–guest complexes because it can form complexes or interact with various materials including proteins [3–6], membrane related substances [7, 8], and host compounds such as cyclodextrins, calixarenes, and cryptophane-A [9–11]. In studying these complexes or interactions the chemical shift of Xe in ^{129}Xe NMR can be utilized as a diagnostic scale because of its exquisite sensitivity to its surroundings. In addition, recent development of laser polarization technique has now increased the ability of

^{129}Xe NMR greatly as a result of sensitivity enhancement of 4–5 orders of magnitude [12]. Utilizing this hyperpolarized (HP) ^{129}Xe gas significant improvement will be made in accuracy and precision as well as ability of high throughput in the analysis of molecular recognition.

Application of HP ^{129}Xe to investigate inclusion complex formation of Xe with guest molecules has been well reviewed by Goodson [12] in basics, but still very few in reported cases. In the present study, we have made an approach to investigate the host–guest complex formation of Xe and water–soluble calixarene by HP ^{129}Xe NMR after exploiting a simple unique graphic method together with a computer method for the analysis of concentration dependence of ^{129}Xe chemical shift. The results are discussed in relation to the energetic aspect as well as the size and solvation effect in the water–soluble complex formation.

Among calixarenes known as one of the hemicarcerand molecule, thiacalixarenes possess sulfide linkage instead of the methylene linkage in conventional

* Author for correspondence. E-mails: sf3j-fktm@asahi-net.or.jp; fujiwara@sahs.med.osaka-u.ac.jp

calixarenes and are interested in the characteristic behavior in the complex formation with metal ions as well as in acid-base properties [13]. 4-Sulfothiacalix[4]arene sodium salt (STCAS) studied in the present study is made water-soluble by replacing the original *tert*-butyl group in thiocalixarenes by sodium sulfonate [14]. Therefore, study of complex formation of STCAS and Xe will be informative for the understanding of Xe-substrate interactions in water. To our knowledge, no studies have been reported for the complex formation of calixarene and Xe in solution.

Experimental

Continuous-flow mode hyperpolarizing system directly connected to NMR spectrometer

The hyperpolarizing system, a modified version of our home-built system reported earlier by Fukutomi *et al.* [15], is connected directly to the NMR spectrometer so that any loss in the degree of polarization is prevented as much as possible while transferring the hyperpolarized (HP) ^{129}Xe gas into a sample solution (Figure 1). A cylindrical glass cell (Pyrex polarizing cell, 6 cm diameter and 20 cm length) was placed in a fringe field (approximately 12 mT) of a super-conducting NMR magnet (9.4 T). A droplet of rubidium (approximately 0.2 g) was deposited into the polarizing cell whose temperature was maintained constant at approximately 110 °C in an oven equipped with a heated-air blower LEISTER CH-6056. A laser diode array (COHERENT Japan Co., FAP-DUO system, 795 nm) was used under 60 W output power. Here the linearly and randomly polarized light from the fiber cable was converted to circularly polarized light through a polarizing unit. The Xe gas can be supplied continuously from the cell through a polyethylene tube to bubble into the sample

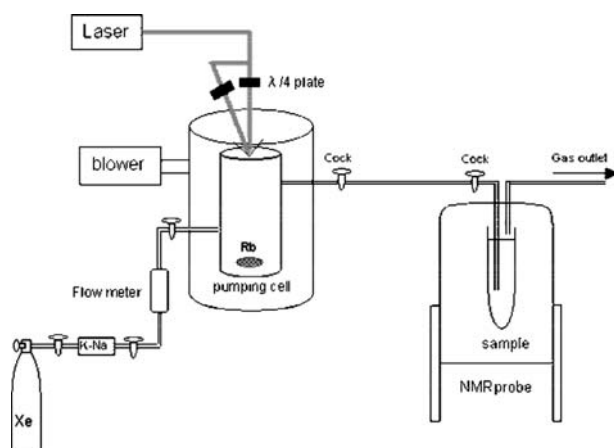


Figure 1. A schematic diagram of the continuous-flow type hyperpolarizing system. The HP ^{129}Xe gas is bubbled into the sample solution from the bottom through a polyethylene tube attached to the stop cock connected to the outlet of the pumping cell.

solution after hyperpolarized to the degree of about 5% in the polarizing cell. The HP ^{129}Xe gas was introduced into the cell at the pressure of a little higher than the atmospheric pressure and finally released to atmosphere under normal pressure after bubbled in the sample solution.

Materials and methods

Natural abundance Xe gas including 26.4% ^{129}Xe , supplied from Japan Air Gases Co. as a standard grade, was used without mixing any foreign gases. 4-Sulfothiacalix[4] arene sodium salt (STCAS) and *p*-phenolsulfonic acid sodium salt (PSAS) were obtained from Tokyo Chemicals Inc. (Figure 2). Deuterium oxide was purchased from Aldrich Co. All organic chemicals were of analytical grade and used as purchased. Sample solutions were made to include variable concentrations of STCAS or PSAS in D_2O . The HP ^{129}Xe gas was bubbled into the sample solution, which was approximately 2.5 ml in volume in a 10 ϕ NMR tube, through a polyethylene tube from the bottom of the solution. The ^{129}Xe NMR chemical shift was measured as bubbling the HP ^{129}Xe gas. ^{129}Xe NMR spectra were recorded on Varian INOVA 400WB NMR spectrometer equipped with a 10 mm double tuned probe. The measurement frequency of ^{129}Xe was 110.6 MHz under the field of 9.4 T. The pulse angle used was 6° with 1 μs pulse width. Other conditions of the NMR measurement were as follows: one FID was acquired under the spectral width of 29 kHz for the number of 10 k points and Fourier transformed after processing with the broadening window function of 30 Hz. The variable temperature experiments were performed with the aid of temperature control unit attached to the spectrometer. Before NMR measurement the sample was kept in the NMR probe for 10 min to attain constant temperature distribution. The sample temperature was tested to be at the desired value prior to the series of measurement with a digital thermometer whose sensor head was immersed in a separate NMR tube containing the same amount of solvent.

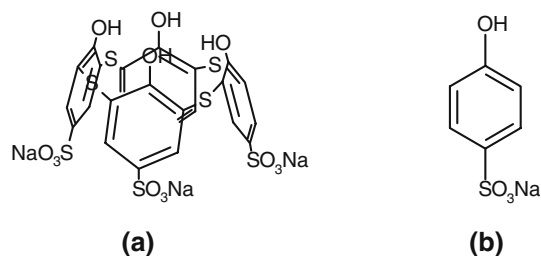


Figure 2. Chemical structure of (a) STCAS and (b) PSAS.

Results

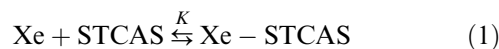
Typical ^{129}Xe NMR spectra for the STCAS solution are shown in Figure 3. Signals appeared near 0 ppm were split into two peaks at 0 and ca. 3 ppm. The high-field peak was confirmed to originate from bubbles in solution, since it disappeared when measurement was repeated after stopping the bubbling of the HP ^{129}Xe gas, and used as reference at 0 ppm; the peak near 3 ppm was assigned to the HP ^{129}Xe gas within the polyethylene tube inserted into the solution. Heights of these two peaks changed from measurement to measurement probably depending on the condition of the bubbling that could change the numbers and location of bubbles affecting the signal intensity picked up by the RF coil.

Shown in Figure 4 is the STCAS concentration dependence of ^{129}Xe chemical shift. When HP ^{129}Xe gas was bubbled into D_2O solution (without STCAS), a peak appeared at 189 ppm for ^{129}Xe dissolved in solution. Then it shifted toward higher field side with adding and increasing the concentration of STCAS: this shift was very large and it amounted as much as 50 ppm for the STCAS 0.3 M solution. This result indicates that very strong special interaction exists between STCAS and Xe. Unlike STCAS only a very little concentration dependence was observed for PSAS. These results show the presence of special interaction between Xe and

STCAS, for which inclusion complex formation is the one that is possible.

Discussion

From the results shown above the concentration dependence observed in Figure 4 for STCAS is interpreted by an inclusion complex formation,



Since only one peak appears in the dissolved state in the present study, Xe is under fast exchange between the free and the included (or bound) states in solution. This is the same case for the inclusion complex formation of Xe and α -cyclodextrin [9]. In contrast, two peaks are observed for the free and bound states in solution in case of the Xe and cryptophane-A [11]. Considering in chemical structure, unlike cryptophane-A, the phenyl rings are flexible in case of STCAS and can be rotated along the axis connecting two sulfur atoms attached to the same ring [16]¹. Such flexibility is prevented in cryptophane-A because of the covered structure in which two units of host, consisting of three phenyl rings, bind together to form a covered cage. This covered

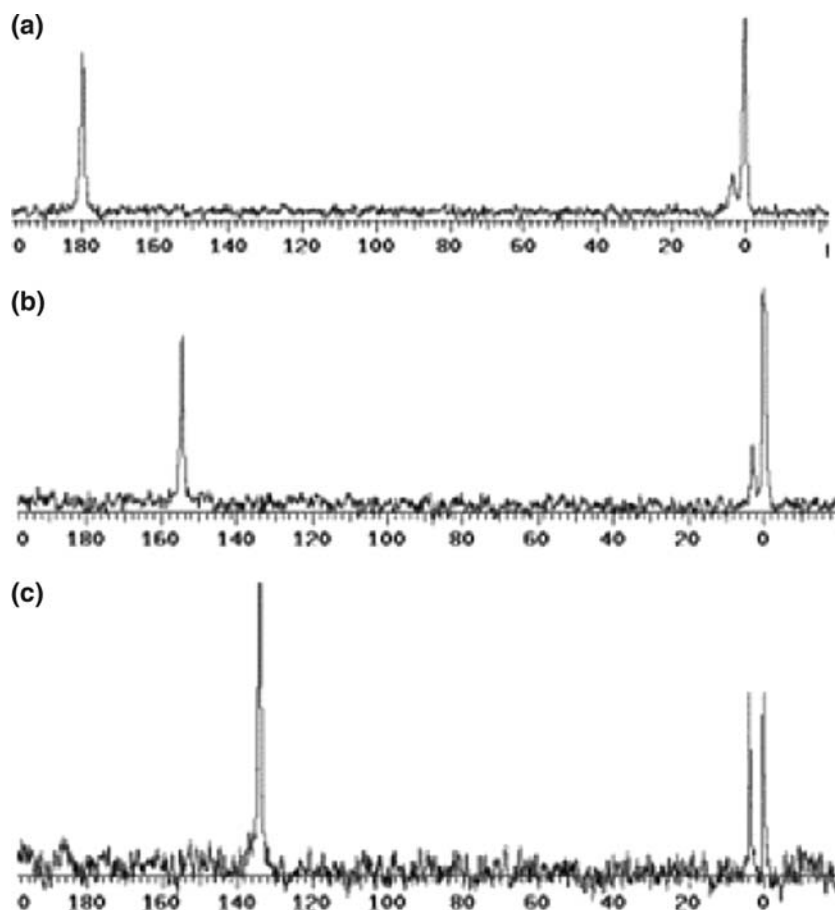


Figure 3. ^{129}Xe -NMR spectra obtained for the STCAS solution. The STCAS concentration is (a) 0.015 M, (b) 0.07 M, and (c) 0.3 M in water.

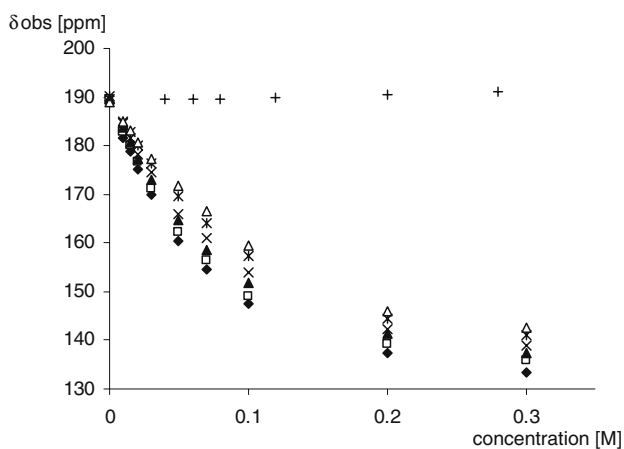


Figure 4. Plots of the ^{129}Xe -NMR chemical shift against the concentration of STCAS. Temperatures of measurement are 25°C (◆), 35 °C (□), 45 °C (▲), 55 °C (×), 65 °C (*), and 75 °C (△). + indicates the data for PSAS, which is used as a reference compound, measured at an ambient temperature.

structure is considered to be responsible for the separated observation of the free and bound state peaks in solution, while it possesses the host windows to open wide enough to allow guests such as ranging from methane to butane to enter and depart [11]. The concentration dependence observed in the present study is about an order larger than that observed in case of Xe and α -cyclodextrin [9], and about 2/3 of that observed for the difference in the two peaks of free and bound states in case of Xe and cryptophane-A [11]. It is interesting to note that the chemical shift changes induced in the inclusion complex formation parallel with the number of phenyl rings included in the host molecules.

Analysis of the concentration dependence on the basis of the chemical equilibrium to derive association constant and bound chemical shift

Under the equilibrium of Equation (1) association constant K is expressed as in Equation (2),

$$K = \frac{[\text{Xe} - \text{STCAS}]}{[\text{Xe}][\text{STCAS}]} \quad (2)$$

and the ^{129}Xe chemical shift can be calculated as the statistical average of the free and the included states under the rapid exchanging condition,

$$\delta_{\text{calcd}} = \frac{[\text{Xe}]\delta_{\text{Xe}} + [\text{Xe} - \text{STCAS}]\delta_{\text{Xe-STCAS}}}{[\text{Xe}] + [\text{Xe} - \text{STCAS}]} \quad (3)$$

where δ_{Xe} and $\delta_{\text{Xe-STCAS}}$ are the chemical shifts in the free and the included states, respectively, and the symbol [] denotes concentration of each species in solution. According to these equations concentration dependent ^{129}Xe chemical shift can be expressed as in Equation (4),

$$\delta_{\text{calcd}} = \frac{\delta_{\text{Xe}} + \{K[\text{STCAS}]_0 / (1 + K[\text{Xe}])\}\delta_{\text{Xe-STCAS}}}{1 + K[\text{STCAS}]_0 / (1 + K[\text{Xe}])} \quad (4)$$

where $[\text{STCAS}]_0$ is the analytical concentration of STCAS:

$$[\text{STCAS}]_0 = [\text{STCAS}] + [\text{Xe} - \text{STCAS}] \quad (5)$$

In the present experiment the HP ^{129}Xe gas is continuously supplied to the sample solution more than 5 min before and during the NMR measurement. Therefore, the concentration of free Xe dissolved in water, $[\text{Xe}]$, is considered to be constant at the saturated value since Xe is always supplied to compensate for the decrease in $[\text{Xe}]$ which would be brought about in progress of the reaction with STCAS when the Xe gas is not supplied continuously. The solubility data are available in reference [17]. In this way analysis of the concentration dependence turns out to be a curve fitting process where the association constant K and $\delta_{\text{Xe-STCAS}}$ are varied to give best fit between the calculated (δ_{calcd}) and observed (δ_{obsd}) values of ^{129}Xe chemical shift throughout the concentration range measured. This is achieved with the aid of a least squares method, and utilized a commercial software ORIGIN from Light Stone Corp in the present case. The results are listed in Table 1. The saturated Xe concentration in water at each temperature is cited from Ref. [17] after a conversion to mol l^{-1} scale from mole fraction scale originally given by the use of the density of water at each temperature. However this temperature dependence does not affect the calculation meaningfully as shown below in the treatment by the graphical method. In fact simulation of the data at 55 °C by using the value of $[\text{Xe}]$ at 25 °C (4.37 mM) instead of the value at 55 °C (2.39 mM) has given the values of $K = 10.8 \pm 0.6 \text{ M}^{-1}$ and $\delta_{\text{Xe-STCAS}} = 120.9 \pm 1.5 \text{ ppm}$ which are well within the limit of estimated errors.

The ^{129}Xe chemical shift is moved toward the high field side by 51 ppm on forming the inclusion complex with STCAS, i.e., $\delta_{\text{Xe-STCAS}} - \delta_{\text{Xe}} = -51.2 \text{ ppm}$, which is much larger than that in case of α -cyclodextrin where $\delta_{\text{Xe-CD}} - \delta_{\text{Xe}} = 2.9 \text{ ppm}$ in water [9], but is about 1/3 of that in the case of cryptophane-A where $\delta_{\text{CRY}} - \delta_{\text{Xe}} = -160 \text{ ppm}$ in $\text{CDCl}_2\text{CDCl}_2$ [11]. These changes in the chemical shift correspond to -13 ppm per phenyl ring in STCAS and -27 ppm per phenyl ring in cryptophane-A. In the case of calix[4]arene inclusion complex, Xe atom is located at a position 4.1–4.3 Å apart from all of the phenyl carbons [10]. Such a large high field shift of -13 to -27 ppm is very hard to explain from the ring current effect of the phenyl ring, whose estimation is given as tables in literature [18] that amounts only 0.3 ppm at a position 4.1 Å apart from the center of the plane of a phenyl ring. Therefore, some distortion of electronic cloud in ^{129}Xe in the cavity of host and/or some specific interaction, such as the electrostatic or charge-transfer nature between Xe and the phenyl ring, can be pointed out as the alternative reason.

Table 1. Analysis of the concentration dependence of ^{129}Xe chemical shift in the inclusion complex formation of STCAS and Xe in water^a

Temperature (°C)	25	35	45	55	65	75
$K [\text{M}^{-1}]$	13.6 ± 0.8	13.0 ± 0.9	11.6 ± 0.6	10.8 ± 0.6	8.3 ± 0.5	6.8 ± 0.6
$\delta_{\text{Xe-STCAS}} [\text{ppm}]$	117.7 ± 1.6	119.8 ± 1.9	120.5 ± 1.5	120.9 ± 1.5	119.3 ± 2.1	117.3 ± 3.0

^a $\delta_{\text{Xe}}[\text{ppm}]$ is confirmed to be slightly temperature dependent: 188.94 (25 °C), 189.56 (35 °C), 189.7 (45 °C), 190.31 (55 °C), 189.71 (65 °C), and 189.09 (75 °C).

Proposition of a simple graphic method for the analysis of the concentration dependence

Analysis of NMR concentration dependence in the interacting system in solution has been reviewed by several authors including simple graphic as well as much sophisticated computer methods, and utility of the NMR spectroscopy is established in the quantitative analysis of the intermolecular interaction such as hydrogen bonding or charge-transfer which may occur in solution [19–21]. In order to search for a new graphic method which is applied simply and readily to the system treated in the present case, where interacting partner is a gaseous compound, Equations (2), (3) and (5) are transformed to the following equation,

$$\frac{1}{\delta_{\text{obsd}} - \delta_{\text{Xe}}} = \left(\frac{1}{K} + [\text{Xe}] \right) \left(\frac{1}{\delta_{\text{Xe-STCAS}} - \delta_{\text{Xe}}} \right) \quad (6)$$

$$\frac{1}{[\text{STCAS}]_0} + \frac{1}{\delta_{\text{Xe-STCAS}} - \delta_{\text{Xe}}}$$

where the symbol δ_{obsd} is used instead of δ_{calcd} in Equation (3) since the observed chemical shift is input to the chemical shift calculated in Equation (3) in the graphic analysis. Equation (6) indicates that a linear relation will be obtained if $\frac{1}{(\delta_{\text{obsd}} - \delta_{\text{Xe}})}$ is plotted against $\frac{1}{[\text{STCAS}]_0}$, and that K and $\delta_{\text{Xe-STCAS}}$ are determined from the slope and intercept of the plot, respectively. As a prerequisite for this linearity concentration of free Xe dissolved in solution, $[\text{Xe}]$, should be constant. This condition has been fulfilled in the present study by supplying Xe gas steadily to the sample solution before 5 min and during the NMR measurement. This plot is shown in Figure 5, which supports good linear relation at all measured temperatures as evidenced by the correlation coefficients larger than 0.99. In these plots the association constant K and $\delta_{\text{Xe-STCAS}}$ are derived from the slope, intercept and $[\text{Xe}]$. For example, K and $\delta_{\text{Xe-STCAS}}$ are determined to be 9.5 M^{-1} and 104.9 ppm , respectively at 25 °C. It is interesting to note that the value of $[\text{Xe}]$, which is equal to 0.00437 M at 25 °C, affects very little to the value of K since $1/K$ is much larger than $[\text{Xe}]$ in the term of slope in Equation (6). The graphic method has given the association constant of 8.2, 7.4, 6.8, 6.1, and 4.9 M^{-1} at 35, 45, 55, 65, and 75 °C, respectively, which are smaller than those obtained from the computer simulation method. Such a systematic discrepancy may be ascribed to the difference in the weighting factor assigned to each data points. That is, experimental values of the chemical shift and

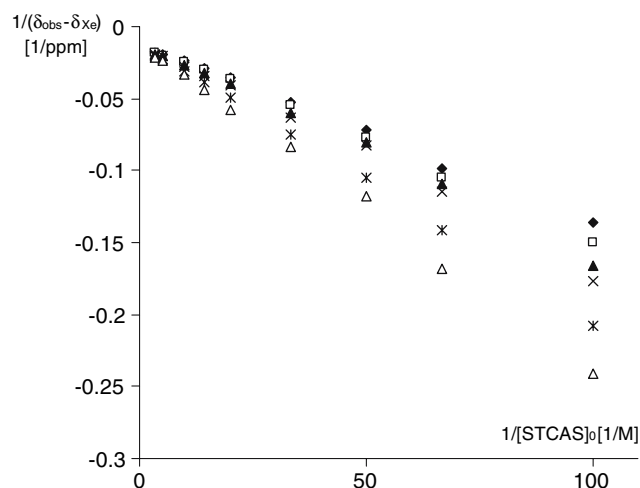


Figure 5. Plots of $1/(\delta_{\text{obsd}} - \delta_{\text{Xe}})$ against $1/[\text{STCAS}]_0$ at (◆) 25 °C, (□) 35 °C, (▲) 45 °C, (×) 55 °C, (*) 65 °C, (△) 75 °C, and PSAS (+) at room temperature. Good linear correlation is obtained corresponding to $r^2 = 0.9962, 0.9998, 0.9996, 0.9946, 0.9991, 0.9998$ at 25, 35, 45, 55, 65, and 75 °C, respectively.

concentration need to be plotted after the necessary transformation in Equation (6), as exemplified in a reciprocal plot. Such a transformation distorts the weighting factor of each data point: for example, the data measured at smaller concentration of STCAS with smaller change in chemical shift are weighted higher and the slope of the linear plot is dominated mainly by the data measured at lower concentrations, i.e., the slope is dominated by the data points located in the right and upper region in Figure 5. On the other hand, each chemical shift datum is weighted evenly in the computer method, and the independent parameters, i.e., K and $\delta_{\text{Xe-STCAS}}$, are adjusted so that the mean squared deviation between the calculated and the observed chemical shifts are minimized. Therefore, in the present study, results from computer method were adopted as final ones, and the graphic method was used for a reference in discussion.

In Table 1 $\delta_{\text{Xe-STCAS}}$ determined from the computer method is found to take a maximum value near 45–55 °C. This tendency is in common with that observed in δ_{Xe} (Table 1). Kawata *et al.* [22] have already reported the ^{129}Xe chemical shift of Xe dissolved in water, δ_{Xe} has shown non-linear and convex parabola-like dependence with temperature [22]. Since such a tendency is only observed in aqueous solution, physical properties of water seem responsible to the phenomenon.

Energetic profiles of the interaction between STCAS and Xe

The association constants determined in the present study are in the similar order to the value reported with α -cyclodextrin in water [9], but clearly smaller than that for cryptophane-A [10]. The cavity volumes are 138, 176, and 81.5 Å³ for calixarene², α -cyclodextrin, and cryptophane-A, respectively while the volume of Xe is 42.2 Å³ corresponding to the diameter of 4.32 Å. Therefore, cryptophane-A fits more favorably with Xe in cavity size and this may be a main reason of high affinity of $K = \sim 3000 \text{ M}^{-1}$. Of course, association constant is strongly dependent on the solvent used as reported for α -cyclodextrin (see Table 2). And hence, comparison should be made preferably in the same solvent. In addition, to allow for the temperature dependence of association constants, stability of the complex formation or affinity of the host–guest molecules had better discussed after measuring the thermodynamic profile of the interaction. This was done for STCAS in the present study. Temperature dependence of the association constant can give thermodynamic parameters of the interaction occurring in solution, which would be useful for understanding the outline of solvation phenomena as well as energetic profiles of the host–guest interaction.

Temperature dependence of the association constant gives the thermodynamic parameters, enthalpy ΔH and entropy ΔS , of the interaction between STCAS and Xe. The van't Hoff plot (Figure 6) according to Equation (7) afforded: $\Delta H = -11.9 \pm 1.9 \text{ kJ mol}^{-1}$ and $\Delta S = -17.4 \pm 5.8 \text{ JK}^{-1} \text{ mol}^{-1}$ (Table 2),

$$\ln K = -\frac{\Delta H}{R} \frac{1}{T} + \frac{\Delta S}{R} \quad (7)$$

where R is the gas constant and T is the absolute temperature. This plot (Figure 6) supports good linear relation as evidenced by the squared multiple correlation coefficient $r^2 = 0.9911$.

According to the idea of enthalpy-entropy compensation relationship [23, 24], systems interacting through similar mechanisms will appear on a similar line in the entropy *versus* enthalpy plots. In addition, the conformational change and the extent of desolvation in host–guest complexation can be derived quantitatively from the slope and the intercept of the $T \Delta S$ *versus* ΔH plot [25]. Interestingly, when $T \Delta S$ vs ΔH plot is made for the

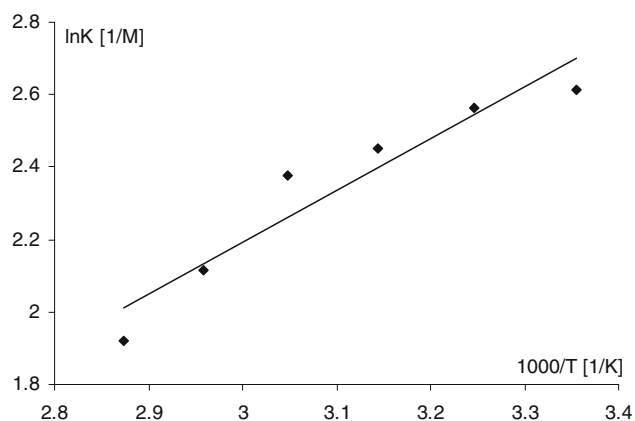


Figure 6. van't Hoff plots of the temperature dependence of association constant for the inclusion complex formation of Xe and STCAS ($r^2 = 0.9911$ for the linear correlation).

data of STCAS–Xe complex including other systems available in literature, the STCAS–Xe system does not so much fit on the calixarene-cation systems but almost fit on the myoglobins–Xe system (Figure 7). This is reasonable since the interaction of Xe with calixarene and myoglobins can be classified in weak-bound and hydrophobic category whereas cation is categorized hydrophilic. This demonstrates a presence of similar driving force, i.e., conformational change and extent of desolvation as well as the type of intermolecular interaction, in between the complexes of STCAS–Xe and myoglobin–Xe.

The extent of desolvation can be discussed in detail from the molecular theory of entropy change on reaction: the entropy change on reaction of Equation (1) can be estimated from molecular theory of thermodynamic functions [26–31]. If the reaction occurs in the ideal gas phase, the entropy change (ΔS_{gas}) is expressed as the difference in standard entropies of the components contributing the reaction,

$$\Delta S_{\text{gas}} = S_{\text{Xe-STCAS}} - S_{\text{Xe}} - S_{\text{STCAS}} \quad (8)$$

where $S_{\text{Xe-STCAS}}$, S_{Xe} , and S_{STCAS} are standard entropies of Xe–STCAS, Xe, and STCAS, respectively. The standard entropy can be calculated as the sum of several contributions including translation, rotation, vibration, and others [26]. Among these contributions those from translational and rotational ones play an important role in the first approximation and they are easily estimated as in Equations (9) and (10) [26],

Table 2. Energetic profiles of the different inclusion complexes of Xe

Substance	$K [\text{M}^{-1}]$	$\Delta H [\text{kJ mol}^{-1}]$	$\Delta S [\text{J K}^{-1} \text{mol}^{-1}]$	Solvent
STCAS	13.6 ± 0.8	-11.9 ± 1.9	-17.4 ± 5.8	Water
Metmyoglobin [2]	146	-30.2	-58.7	Water
Myoglobin [2]	94	-21.4	-33.5	Water
Cyanomyoglobin [2]	145	-37.7	-83.8	Water
Cryptophane-A [9]	ca. 3000 (5 °C)			$\text{CDCl}_2\text{CDCl}_2$
α -Cyclodextrin [7]	2.28 (25 °C)			DMSO
α -Cyclodextrin [7]	22.9 (25 °C)			Water

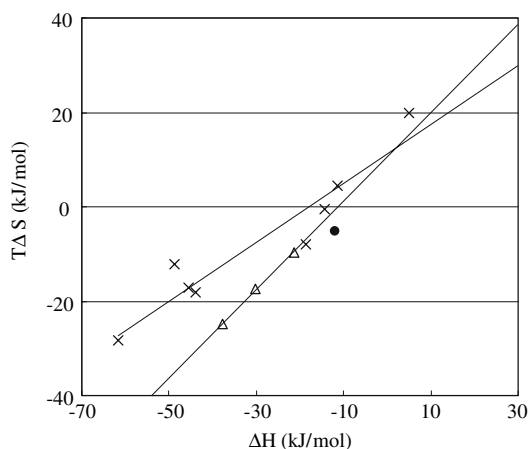


Figure 7. $\Delta H - T \Delta S$ plots for the complex formation of calixarenes and cations (x) [24] as well as myoglobins and Xe (Δ) [2]. Cations included are Li^+ , Na^+ , K^+ , Rb^+ , and Cs^+ . • indicates the data of the present study for the complex formation of STCAS and Xe.

$$S_{\text{tr}} = R(1.5 \ln M + 2.5 \ln T - \ln P - 1.1650) \quad (9)$$

$$S_{\text{rot}} = R(0.5 \ln I_A I_B I_C + 1.5 \ln T - \ln \sigma - 2.7106) \quad (10)$$

where M is the molecular weight, P is the pressure, I is the moment of inertia, and σ is the symmetry number. Such a model was successfully applied to discuss solvation effect in the reaction in solution [27, 28, 30, 31]. Since two molecules bind to one molecule in Equation (1), ΔS_{gas} calculated as in Equation (8) will be negative and large in absolute value.³ In fact, the term including $I_A I_B I_C$ in Equation (10) will contribute less to ΔS_{gas} since the moment of inertia is not expected to change drastically in the present case whether Xe atom presents in the center of STCAS or not. In this way a simple calculation predicts the ideal gas value of $\Delta S_{\text{gas}} = -216.4 \text{ JK}^{-1} \text{ mol}^{-1}$ for reaction (1), whereas the experimental value observed in the present study is $-17.4 \text{ JK}^{-1} \text{ mol}^{-1}$. This value, $-17.4 \text{ JK}^{-1} \text{ mol}^{-1}$, is similar to those observed for α -cyclodextrin and cyclohexanol,³ where 2.0 to $-14 \text{ JK}^{-1} \text{ mol}^{-1}$ is reported for ΔS in solution and 1.6–1.3 molecules of water are predicted to be released in the inclusion complex formation. Therefore, a release of similar number of water molecules is suggested in the present case in the inclusion complex formation of STCAS and Xe.

Model of the association of STCAS with Xe

Bartik *et al.* [9] have proposed a three-site model for the complex formation of Xe with α -cyclodextrin, in which non-complexed fraction of Xe is assumed to be distributed in close environment of cyclodextrin and in bulk solvent. This model was introduced to explain their observation that the ^{129}Xe chemical shift changes with the concentration of the host molecule in somewhat different manner as expected for the simple model of 1:1 complex formation. In the present study,

however, the observed changes in the chemical shift are straightforward as expected from the simple model of 1:1 complex formation and the simple analysis has resulted in a straight line in the graphic method. Therefore, three-site model is not necessary for the interpretation and not discussed further in the present study.

In case of myoglobins, for which four Xe sites of occupancy from 0.45 to 1.0 have been evidenced by X-ray crystallography [6], the association constant has been estimated for the complex formation of 1 (myoglobin):2 (Xe) complex as well as the 1 (myoglobin):1 (Xe) complex in solution [4]. In case of calixarene [10], formation of 1:1 complex is assumed in common with the present study. Successful derivation of the association constant as well as the bound chemical shift together with the successful estimation of thermodynamic parameters supports the assumption of 1:1 complex formation in solution in the present study.

In regard to the geometry of inclusion complex the SPINOE (Spin Polarization-Induced Nuclear Overhauser Effect) experiment as reported for the Xe complex with cryptophane-A or α -cyclodextrin [12, 32, 33] could give important information including dynamic profile of the calixarene ring inversion. But a detailed three-dimensional analysis of the conformation has been prevented from the insufficient number of geometrical constraints provided from the very simple ^1H spin system in calixarene studied in the present study.

Conclusion

The hyperpolarized ^{129}Xe NMR spectroscopy has been successfully applied to investigate the inclusion complex formation between Xe and 4-Sulfothiacalix[4]arene sodium salt (STCAS) in water by using our new system which can supply hyperpolarized ^{129}Xe gas continuously to a sample tube directly. The STCAS molecule was shown to move the ^{129}Xe chemical shift toward the high field side by 51 ppm. As a feasible method of analysis of the concentration dependence of ^{129}Xe chemical shift, graphical method has been proposed together with much sophisticated computer method. The association constant are determined to be $13.6 \pm 0.8 \text{ M}^{-1}$ at 25 °C. In addition, the temperature dependence of the association constant provided the thermodynamic parameter of enthalpy (ΔH) and entropy (ΔS): $\Delta H = -11.9 \pm 1.9 \text{ kJ mol}^{-1}$ and $\Delta S = -17.4 \pm 5.8 \text{ JK}^{-1} \text{ mol}^{-1}$. These parameters are essential in discussing the intermolecular interaction in solution quantitatively. The entropy value suggests a release of solvent water molecule(s) on the formation of the inclusion complex.

Since our methodology of the hyperpolarized ^{129}Xe NMR spectroscopy system and analysis of experimental data has advantages in efficiency, accuracy and simplicity, more precious and feasible analysis can be applied to various solute–solvent interactions of Xe with different substrates in solution including proteins related

to general anesthesia or those with importance in supramolecular chemistry.

Notes

1. In our ^1H NMR spectra measured in 1 mM STCAS solution in D_2O a singlet peak appeared in the aromatic region at 7.794 ppm, and no evidence was obtained about the possible calixarene ring inversion as reported in the related compounds [16, 34]. In addition, this chemical shift was not changed on bubbling of the HP ^{129}Xe gas, and difficulty of observing the inclusion complex formation from ^1H NMR spectra was realized.
2. The value for calixarene is calculated from the crystallographic data [10].
3. For example, $\Delta S = -253.1 \text{ JK}^{-1} \text{ mol}^{-1}$ is calculated for the ideal gas-phase reaction of a tin compound of $\text{CH}_3\text{SnCl}_3 + \text{DMSO} = \text{CHSnCl}_3 \cdot \text{DMSO}$, where two molecules bind to one molecule resulting in a reduction of the translational entropy of one molecule [30].

References

1. (a) N.P. Franks and W.R. Lieb: *Nature* **367**, 607 (1994). (b) N.P. Franks, R. Dickinson, S.L.M. de Sousa, A.C. Hall, and W.R. Lieb: *Nature* **396**, 324 (1998).
2. J.M. Lehn: *Supramolecular Chemistry. Concepts and Perspectives*, VCH, Weinheim, (1995).
3. B.P. Schoenborn, H.C. Watson, and J.C. Kendrew: *Nature* **207**, 28 (1965).
4. G.J. Ewing and S. Maestas: *J. Phys. Chem.* **74**, 2341 (1970).
5. R.F. Tilton Jr. and I.D. Kuntz Jr.: *Biochemistry* **21**, 6850 (1982).
6. R.F. Tilton Jr., I.D. Kuntz Jr., and G.A. Petsko: *Biochemistry* **23**, 2849 (1984).
7. S. Mckim and J.F. Hinton: *Biochim. Biophys. Acta.* **1193**, 186 (1994).
8. Y. Xu and P. Tang: *Biochim. Biophys. Acta.* **1323**, 154 (1997).
9. K. Bartik, M. Luhmer, S.J. Heyes, R. Ottinger, and J. Reisse: *J. Magn. Reson. B* **109**, 164 (1995).
10. E.B. Brouwer, G.D. Enright, and J.S. Ripmeester: *J. Chem. Soc., Chem. Comm.* 939 (1997).
11. K. Bartik, M. Luhmer, J.-P. Dutasta, A. Collet, and J. Reisse: *J. Am. Chem. Soc.* **120**, 784 (1998).
12. B.M. Goodson: *J. Magn. Reson.* **155**, 157 (2002).
13. H. Matsumiya, Y. Terazono, N. Iki, and S. Miyano: *J. Chem. Soc., Perkin. Trans.* **2**, 1166 (2002).
14. N. Iki, T. Fujimoto, and S. Miyano: *Chem. Lett.* 625 (1998).
15. J. Fukutomi, E. Suzuki, T. Shimizu, A. Kimura, and H. Fujiwara: *J. Magn. Reson.* **160**, 26 (2003).
16. J. Lang, J. Vlach, H. Dvoráková, P. Lhoták, M. Himl, R. Hrabal, and I. Stibor: *J. Chem. Soc., Perkin Trans.* **2**, 576 (2001).
17. H.L. Clever: *Solubility Data Series, vol.2*; IUPAC Anal. Chem. Div., Pergamon Press. (1979).
18. C.W. Haigh and R.B. Mallon: *Org. Magn. Reson.* **4**, 203 (1972).
19. J.C. Davis Jr. and K.K. Deb: *Adv. Magn. Reson.* **4**, 201 (1970).
20. R. Macomber: *J. Chem. Educ.* **69**, 375 (1992).
21. R. Foster: *Organic Charge Transfer Complexes*, Academic Press, London (1969), pp. 125–215.
22. Y. Kawata, T. Kamiya, H. Miura, A. Kimura, and H. Fujiwara: *Int. Congress Ser.* **1265**, 172 (2004).
23. J. Lefler and E. Grunwald: *Rates and Equilibrium of organic Reactions*, Wiley-Interscience, New York (1963), pp. 315–402.
24. S.W. Benson: *Thermochemical Kinetics: Methods for the Estimation of Thermodynamical Data and Rate Parameters*, 2nd ed., Wiley, New York (1976), pp. 1–77.
25. Y. Inoue and T. Wada: *Adv. Supra. Chem.* **4**, 55 (1997).
26. G. Herzberg: *Molecular Spectra and Molecular Structure II, Infrared and Raman Spectra of Polyatomic Molecules*, Van Nostrand, New York (1945), pp. 501–537.
27. G.H. Nancollas: *Quart. Rev.* **14**, 402 (1960).
28. I. Tabushi, Y. Kiyosuke, T. Sugimoto, and K. Yamamura: *J. Am. Chem. Soc.* **100**, 916 (1978).
29. J.F. Wojcik: *Bioorg. Chem.* **12**, 130 (1984).
30. H. Fujiwara, F. Sakai, A. Kawamura, N. Shimizu, and Y. Sasaki: *Bull. Chem. Soc. Jpn.* **58**, 2331 (1985).
31. H. Fujiwara, H. Arakawa, S. Murata, and Y. Sasaki: *Bull. Chem. Soc. Jpn.* **60**, 3891 (1987).
32. M. Luhmer, B.M. Goodson, Y.-Q. Song, D.D. Laws, L. Kaiser, M.C. Cyrier, and A. Pines: *J. Am. Chem. Soc.* **121**, 3502 (1999).
33. Y.-Q. Song, B.M. Goodson, R.E. Taylor, D.D. Laws, G. Navon, and A. Pines: *Angew. Chem. Intl. Ed. Engl.* **36**, 2368 (1997).
34. S. Shinkai, K. Araki, T. Matsuda, and O. Manabe: *Bull. Chem. Soc. Jpn.* **62**, 3856 (1989).